

EXPERIMENTAL STUDY ON THE PHASE VELOCITY OF WIND WAVES PART: 2 OCEAN WAVES

Kuo, Yi-Yu
Hydraulic Civil Engineering, Faculty of Engineering, Kyushu University : Graduate student

Mitsuyasu, Hisashi
Research Institute for Applied Mechanics, Kyushu university : Professor

Masuda, Akira
Research Institute for Applied Mechanics, Kyushu University : Research Associate

<https://doi.org/10.5109/6617925>

出版情報 : Reports of Research Institute for Applied Mechanics. 27 (84), pp.47-66, 1979-09. 九州大学応用力学研究所
バージョン :
権利関係 :



**EXPERIMENTAL STUDY ON THE PHASE VELOCITY
OF WIND WAVES
PART 2 OCEAN WAVES**

By Yi-Yu KUO*, Hisashi MITSUYASU**
and Akira MASUDA***

Ocean waves are measured at an oceanographic research tower using a triangular array of wave gauges. The propagation direction and the phase velocity of spectral components of waves are determined from observed cross spectra. It is shown that observed phase velocity and coherence of spectral components of ocean waves are consistent with a linear theory of two-dimensional random waves. Slight differences between the linear theory and the observations are attributed approximately to the effects of weak opposing waves reflected from coastal area.

Key words: Ocean waves, Phase velocity, Angular distribution, Reflected waves

1. Introduction

In a series of our recent papers, we have studied phase velocities of spectral components of wind-generated waves (Masuda et al. 1979, Mitsuyasu et al. 1979 and Kuo et al. 1979, hereinafter referred to as I, II and III). In I, a theoretical framework was given, upon which to examine the dispersion relation of random gravity waves; a weakly nonlinear theory was developed to the third order for a statistically stationary and homogeneous field of random gravity waves.

The papers II and III were concerned with experimental studies on the dispersion relation of wind-generated waves. In II, random waves were generated by wind in the first half of a wind-wave flume and the latter half of the flume was kept free from the wind to measure the waves unaffected by the wind and wind-generated drift current. The phase velocity and coherence of spectral components of random waves in the latter area were

* Graduate student of Hydraulic Civil Engineering, Faculty of Engineering, Kyushu University

** Professor, Research Institute for Applied Mechanics, Kyushu University

*** Research Associate, Research Institute for Applied Mechanics, Kyushu University

determined by a usual technique of the cross-spectral analysis. The data showed good agreements with the nonlinear theory developed in I, and observed characteristics of the phase velocity and the coherence of the spectral component were attributed to the effects of the nonlinearity and angular spreading of random waves. Particularly, in a dominant frequency range ($0.7f_m \leq f \leq 1.6f_m$) near the spectral peak frequency f_m , observed data agreed also fairly well with the linear theory. In III, wind-generated waves were measured in a generation area of the wind-wave flume which was the same to that used in II. The phase velocity and the coherence of the spectral component were determined with the same technique as that in II and were compared with the predictions of a linear theory where the effects of the angular spreading and the drift current were taken into account. Fairly good agreements between the linear theory and the experiment were obtained again in the dominant frequency range $0.7f_m \sim 1.6f_m$, where most of the spectral energy was contained. However, due to difficulties in the nonlinear theory of random waves co-existing with the drift current, we reserved the theoretical analysis of the observed data in a high frequency region $f > 1.6f_m$, where the nonlinear effects are remarkable.

The present study is a sequel to those studies mentioned above. The phase velocity of the spectral component of ocean waves is studied through the analysis of wave data measured at an oceanographic research tower.

Due to the technical difficulties, quite a few studies have been made on the phase velocity of ocean waves. As far as we know, Yefimov et al. (1972) is the only study which is similar to our present study. Their data obtained in an open littoral area of the Black Sea show remarkable deviations from the predictions of the linear theory for high frequencies, which are similar to our previous results in a laboratory flume (II and III). In detailed points, however, their results are slightly different from ours presented in II and III.

In the measurement of the phase velocity of ocean waves, some difficulties arise from the fact that the dominant direction of the wave field is not known beforehand and depends on the generating conditions of the waves. Therefore, we have to determine the wave direction and the phase velocity simultaneously. Yefimov et al. (1972) used one pair of two wave gauges aligned to the direction of the mean wind and the visible direction of wave propagation. However, if the wave direction is different from the visible direction of wave propagation, some errors will be introduced into the measured phase velocity. In the present study we use three pairs of wave data measured simultaneously with triangular array of wave gauges. The propagation direction and the phase velocity of spectral component are simultaneously determined from three pairs of cross spectra. This problem will be investigated first, and then measured phase velocities and coherences of spectral components will be discussed.

2. Wave observation

Ocean waves were measured at an oceanographic research tower located 2km northwest of Tsuyazaki port, which faces on the Tsushima strait (Figure 1). The water depth at the station is 15.5m and the slope of the sea floor around the tower is relatively gentle ($\sim 1/300$).

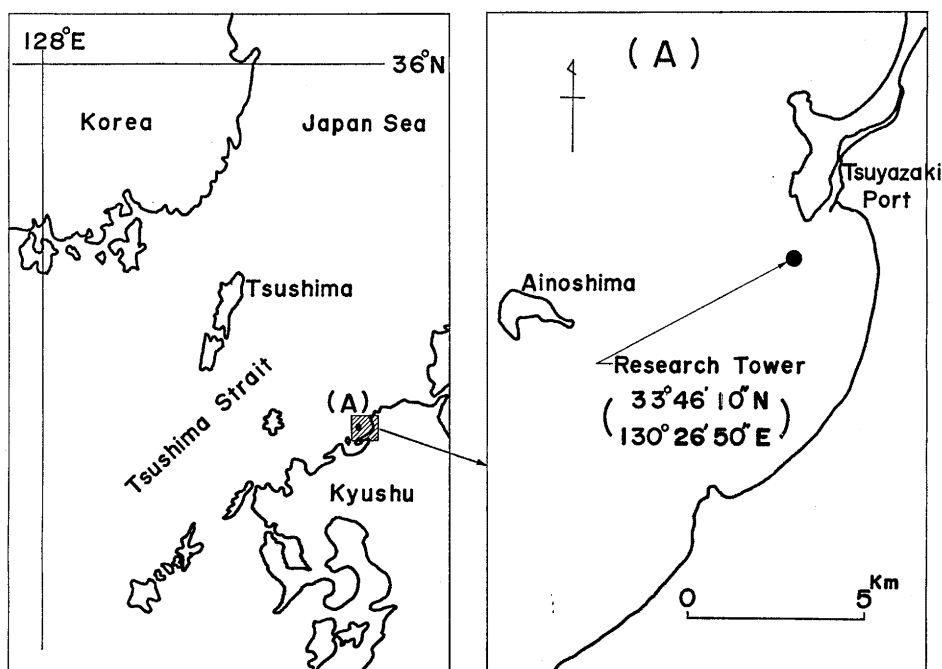


Figure 1 Location of oceanographic research tower

The observation tower is a simple equilaterally triangular platform which is composed essentially of three vertical piles (diameter 0.8m) driven into the sea bottom at 7m distances from one another. Waves were measured by three capacitance-type wave gauges fixed to each pile of the tower with arms 1m long so as to reduce the effects of the disturbances from the vertical piles. The wave gauges form an equilaterally triangular array of side 7m and can detect directional properties as well as the surface elevation. Wind speed and wind direction were measured by a wind vane located at the top of the tower, the height of which is 12.5m above the sea surface. The details of the observation facility and equipments have been described in another paper (Tasai et al. 1977).

Waves were measured simultaneously with the three wave gauges and recorded on a tape-recorder of casset-type in a digital form with sampling

frequency 10Hz. In routine observations, measurement is controlled automatically; with time interval of 2 hours, the system records waves for 20 minutes only if the wind speed is larger than an assigned value (usually 7m/s). In some cases, wave records of the same length are obtained at an assigned time interval irrespective of the wind speed in order to study swells or waves under very weak wind.

Wind speed and wind direction are recorded on a multipoint strip-chart recorder for every two hours. Measurement of the wind and wave at the observation tower has been made since 1975.

In order to study the phase velocity of ocean waves we have analysed about 30 wave data. In the present paper, however, only three typical data including the wind-generated waves and swell are mainly discussed, because the other data show the similar properties.

The meteorological conditions and the characteristic properties of these three wave data are shown in Table 1. Wave data No. 1 and No. 3 correspond to waves generated by the wind which had been blowing steadily over ten hours before measurement. On the other hand, wave data No. 2 seems to be those of the swell, because it has low spectral peak frequency in spite of the very low wind speed.

Table-1: Meteorological conditions and properties of ocean waves.
 f_m : spectral peak frequency, $H_{\frac{1}{3}}$: significant wave height,
 E: total wave energy, L_m : wave length corresponding to
 the frequency f_m .

Wave No.	Date	Time	Wind speed (m/s)	Wind direction (N°)	f_m (Hz)	$H_{\frac{1}{3}}$ (m)	E (m ²)	$H_{\frac{1}{3}}/L_m$	Remarks
1	Oct. 29, 1976	2:35	8.7	327°	0.15	1.72	0.186	0.0238	Wind wave
2	Oct. 30, 1976	14:37	1.0	278°	0.08	0.75	0.036	0.0031	Swell
3	Dec. 9, 1977	5:35	7.8	288°	0.21	1.07	0.072	0.0304	Wind wave

3. Analysis of the wave data

3.1 Analysis of power spectra and cross spectra

The wave data recorded on caset tapes were transferred to magnetic tapes for computer use. In the present analysis, the data corresponding to the initial 5 minutes were discarded in each case and remaining data of 15 minutes were used. As mentioned previously, the sampling frequency of the data is 10Hz and the Nyquist frequency of the wave spectra is 5Hz. Each of the wave data was divided into 4 sub-samples of 204.8 sec which con-

tained 2048 data points. Since the spectral density of ocean wave varies very rapidly in the low frequency part of the spectrum, we used the data window of the type of cosine bell in order to avoid the leakage error in the discrete Fourier transformation.

The spectral analysis of the wave data was done on a FACOM 230-48 computer using a standard program based on fast Fourier transform procedures. In order to calculate the phase velocity of the spectral component, cross spectra were also computed for each pair of wave gauges. Then, the three wave gauges give three cross-spectra. Final data of the power spectra and the cross spectra were obtained by taking sample mean of four sub-samples of raw wave spectra and taking moving average of successive five line spectra. Therefore, equivalent degrees of freedom of the measured spectra are approximately 40.

From the cross spectrum of waves

$$Cr_{i,j}(\omega) = CO_{i,j}(\omega) - iQU_{i,j}(\omega), \quad (1)$$

we obtain the phase lag $\bar{\theta}(\omega)$ and the coherence $Coh(\omega)$ as

$$\bar{\theta}_{i,j}(\omega) = \tan^{-1}[QU_{i,j}(\omega)/CO_{i,j}(\omega)], \quad (2)$$

and
$$Coh_{i,j}(\omega) = \{[QU_{i,j}^2(\omega) + CO_{i,j}^2(\omega)]/\phi_i(\omega)\phi_j(\omega)\}^{\frac{1}{2}}, \quad (3)$$

where ω is the (angular) frequency. The suffix " i, j " corresponds to the wave data obtained respectively with the wave gauges i and j , and ϕ_i is the power spectrum of waves measured with the wave gauge i .

3.2 Method for determining the phase speed

The central problem is to find the phase speed of wind waves by use of three observed cross spectra $Cr_{i,j}(\omega)$. These informations are too few to give the dispersion relation, so that they must be supplemented by a simple model which necessarily contains several assumptions.

First, consider an ideal model in which all waves of a frequency ω propagate with a phase speed $C(\omega)$ in one direction $\alpha(\omega)$. Then we have three equations

$$C(\omega) = \omega l \cos(\beta_{i,j} - \alpha(\omega)) / \bar{\theta}_{i,j}(\omega), \quad (4)$$

where $\beta_{i,j}$ denotes the direction from the wave gauge i toward the gauge j and l ($=7m$) the distance between them. For the determination of the two unknowns $C(\omega)$ and $\alpha(\omega)$, two independent equations are necessary and sufficient. We may take any two of equations (4) for this purpose. Although there are three pairs of equations on which to calculate C and α (we call them "basic couples"), any of them will give the same solutions.

However, waves may propagate with different phase speeds and in various directions, so that equations (4) are not exact any more. When we

dare to determine C and α in the above mentioned manner, we will find, in general, three different results dependent on the basic couple. Even in such a situation, if approximately the same C and α are obtained irrespective of the basic couple, the ideal model might not be invalid. More strongly, let us suppose that if the three basic couples yield nearly equal C and α , the model holds at least in the approximate sense: waves of this frequency propagate with the phase speed $C(\omega)$ in the direction $\alpha(\omega)$. For such frequencies as give inconsistent C or α , we refrain ourselves from determining the phase speed and the wave direction. This is the fundamental procedure by which we obtain approximate solutions of this difficult problem using only three cross-spectra.

Now we extend the ideal model and make a more reasonable and realistic one by introducing the directional distribution. That is, we suppose that for a fixed frequency ω , waves propagate with a phase velocity $C(\omega)$ in various directions but the directional distribution takes the form

$$S(\omega, \theta) \begin{cases} = \frac{1}{\sqrt{\pi}} \cdot \frac{\Gamma(1+m/2)}{\Gamma(1/2+m/2)} \cdot \cos^m(\theta - \alpha(\omega)) & \text{for } |\theta - \alpha| \leq \frac{\pi}{2} \\ = 0 & \text{otherwise,} \end{cases} \quad (5)$$

where $\alpha(\omega)$ means the main direction, Γ denotes the gamma function and m is assumed appropriately. We call this model as the "realistic" one. If $\alpha(\omega)$ is known, it enables us to define "pseudo" phase speeds by

$$\tilde{C}_{i,j}(\omega) = \omega l \cos(\beta_{i,j} - \alpha(\omega)) / \tilde{\theta}_{i,j} \quad (6)$$

in the analogous form to (4). It must be kept in mind that "pseudo" phase velocities $\tilde{C}_{i,j}(\omega)$ are not equal to the "true" phase $C(\omega)$ even if the model holds exactly*), and that $\tilde{C}_{i,j}(\omega)$ may differ from one another. Appendix A shows this situation. Moreover, it reveals that $\tilde{C}_{i,j}(\omega) (\neq C(\omega))$ approximately agree with one another when $k(\omega)l$ is small, where $k(\omega)$ is the "true" wavenumber defined from the "true" phase speed by $k(\omega) \equiv \omega/C(\omega)$. Therefore we may adopt the same procedure as in the ideal model for small kl .

Once the main direction $\alpha(\omega)$ is determined in that way, the realistic model permits us to calculate "theoretical" "pseudo" phase speeds and "theoretical" coherences if the "true" phase speed $C(\omega)$ is assumed appropriately. Then, they are compared with "observe" "pseudo" phase velocities and "observed" coherences. Thus we can examine the validity of the model though indirectly.

In what follows, we investigate only the realistic model with the linear

*) This is the reason why we have introduced a new word "pseudo" phase speed.

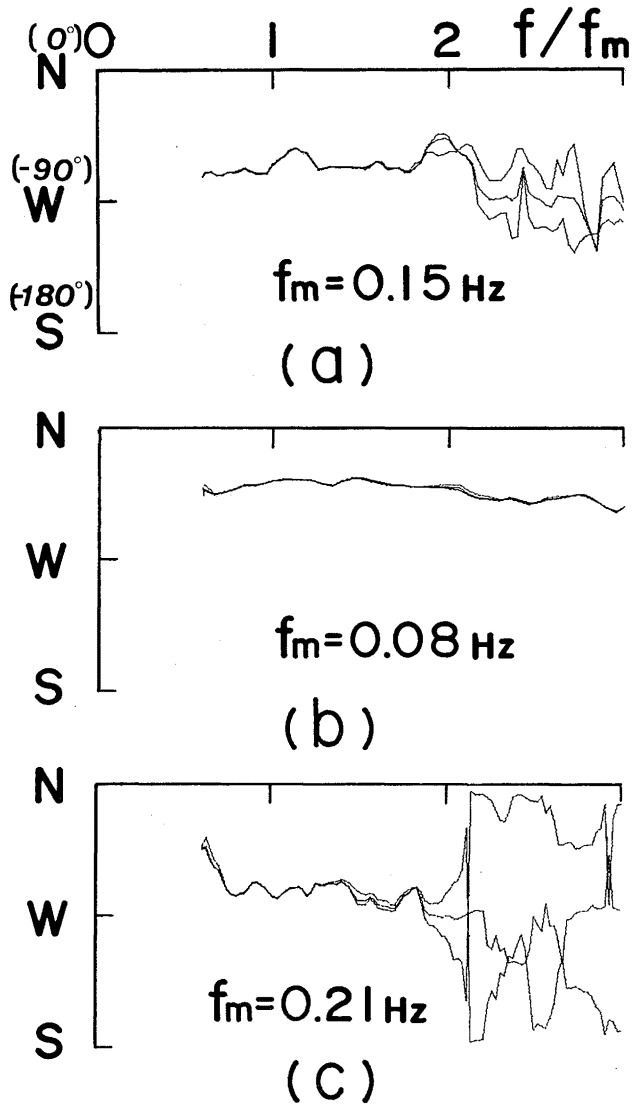


Figure 2 Comparisons of three solutions for the main direction of wave propagation $\alpha(f)$ based on the three basic couples of equation (6).
 (a) wave data No.1 (b) wave data No.2
 (c) wave data No.3

dispersion relation $C(\omega) = C_0(\omega)^*$. Namely, the usual two-dimensional model of random linear waves with the directional distribution of $\cos^m \theta$ -type (See Appendix A for details). The terms "pseudo" and "true", are omitted hereafter for simplicity and for consistency with our previous papers, unless it becomes necessary to distinguish between them.

4. Results and discussions

4.1 Main directions

Three solutions of the main direction α based on the three basic couples are shown in the same figures (Figure 2) as functions of the normalized frequency f/f_m , where f_m denotes the spectral peak frequency. They agree with one another within a frequency range from $0.6f_m$ up to 0.3Hz for each case. Note that the lower bound ($0.6f_m$) of this consistency range depends on the spectral peak frequency, while the upper bound (0.3Hz) not. Outside of this range, the main direction α is not determined consistently by our method. For lower frequencies ($\leq 0.6f_m$) inconsistency probably arises from such low spectral densities as are comparable with electric noises and make data analysis inaccurate. For higher frequencies the disagreement of the three solutions perhaps comes from the method in use. As shown in Appendix A, our procedure does not assure the unique α independent of the basic couples for large $k(\omega)l = \omega l/c(\omega)$. Appendix A also tells us that if we assume the linear dispersion relation and moderate directional distributions ($m=4$), f_c roughly corresponds to 0.3Hz , where f_c is such a critical frequency that the present method does not yield consistent $\tilde{\alpha}$ or α for frequencies larger than f_c . For ordinary directional distributions f_c depends mainly on the distance l , which is constant in our observational conditions. The above argument suggests that a smaller array of wave gauges may allow a broader consistency range.

It is to be noticed that within the consistency range, $\alpha(\omega)$ in each case takes an almost constant value $\bar{\alpha}$ with deviation of 15° at most. This is likely to occur, since the main direction $\alpha(\omega)$ of waves usually agrees with that of winds. Observationally, the representative main directions $\bar{\alpha}$ differ from mean wind directions shown in Table-1 by amount of about 20° for data No.1, 45° for data No.2 and 0° for data No.3. The discrepancy found except in the last case seems to bring no serious problems; for data No.1, though $\bar{\alpha}$ does not coincide to the mean wind direction observed at the time of wave measurement, it agrees with that observed two hours before; the second case corresponds to swells, which originate in the far distance and have no direct relation with the very weak wind blowing around

*¹ Here, C_0 is the phase velocity of long-crested linear waves of wave length L in a finite depth h , which is given by $C_0(\omega) = \frac{g}{\omega} \tanh\left(\frac{2\pi h}{L}\right)$.

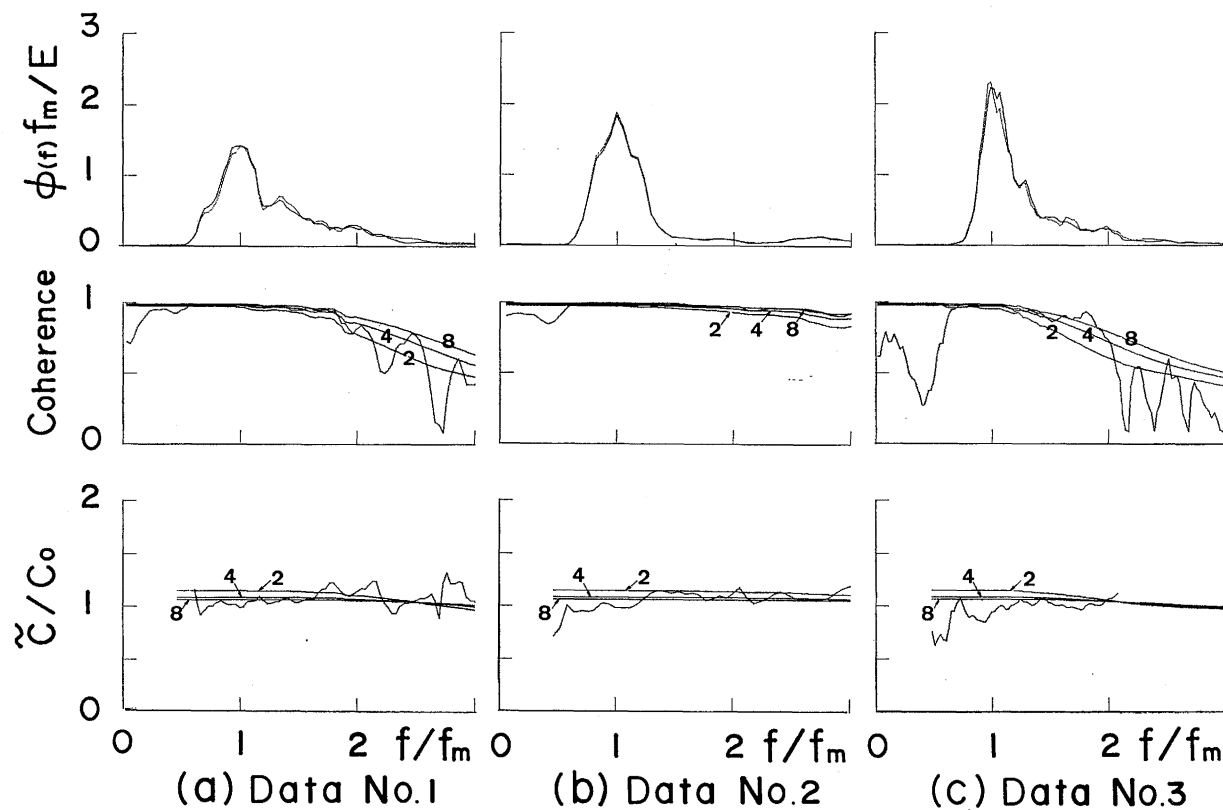


Figure 3, Power spectrum (normalized), coherence and phase velocity (normalized) obtained with wave gauges 2 and 3 (rugged curve). Smooth curves marked with 2,4,8 are the predictions of the linear theory where the angular distribution function is assumed as $S(\theta) \sim \cos^m \theta$, $m=2, 4, 8$.

the observation point.

Thus we reasonably assume $\alpha(\omega) = \alpha(2\pi \times 0.3)$ for $\omega \geq 2\pi \times 0.3$ when it is necessary to determine the observed (pseudo) phase speed or to calculate the theoretical (pseudo) phase speed and theoretical coherence for those frequencies.

In the following, we examine often only the data based on the pair of wave gauges 2 and 3 for simplicity. This pair is selected because it has the direction closest to the representative wave direction $\bar{\alpha}$ and consequently shows the highest coherence for every case of the data. (See Appendix A for another reason.)

4.2 Power spectrum

At the top of Figures 3a, b and c, the normalized spectra $\phi_i f_m / E (i=2, 3)$ are shown as functions of the normalized frequency f/f_m . It can be seen that the two power spectra ϕ_2 and ϕ_3 almost coincide with each other. The spectral form in 3a (wave data No. 1) is fairly close to the Pierson-Moskowitz spectrum, and that in 3c (wave data No. 3) to the JONSWAP spectrum with $\gamma=2.0$. However, the spectral form in 3b (wave data No. 2), which corresponds to swells, has little resemblance to the both standard forms.

Generally, the steepness of ocean waves is not as large as that of laboratory wind waves and the nonlinearity of ocean waves are considered not so large. However, since the phase velocity measured by the cross-spectral technique is sensitive to the nonlinear forced waves (Mitsuyasu et al 1979), it is better to estimate the order of the magnitude of forced wave components for the case of wave data No. 3, which has the largest wave steepness among the present data. Following the method described in our previous

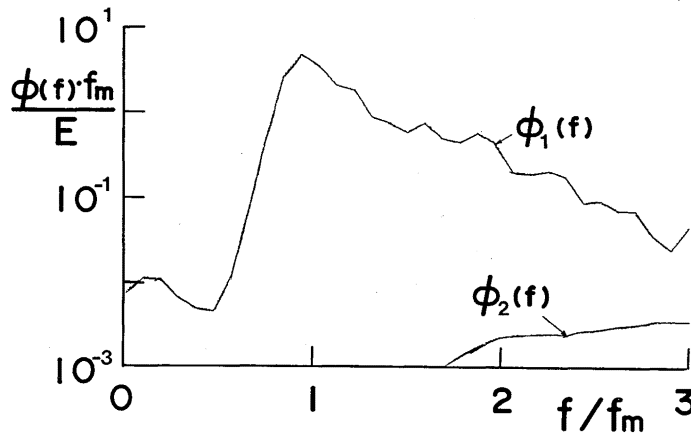


Figure 4 Normalized power spectra of free wave ϕ_1 and forced wave ϕ_2 .

paper (Masuda et al 1979), we calculate the power spectrum of forced waves by taking the angular distribution function of the form $\cos^4\theta$. As shown in Figure 4, the spectral density of the forced waves is negligibly small; about 1% of free waves. The effect of forced wave components on the phase velocity will be discussed later in § 4.4.

4.3 Coherence

The coherence of waves measured at two wave gauges decreases with the increase of kl , where k is the wavenumber. If the distance l between two wave gauges is fixed as in our case, the coherence decreases with frequency f under the condition that f increases with k . (See Appendix A for details). A knowledge of these general features are indispensable in understanding the following behavior of the observed coherences.

Figures 5a, b and c show the observed coherences (rugged curves) for wave data No.1, No.2 and No.3 respectively. The top, middle and bottom figures correspond respectively to the pairs of wave gauges 1-2, 2-3 and 3-1. The coherences based on the wave gauges 2 and 3 have been shown also at the middle of Figures 3a, b and c. The coherence is approximately unity near the frequency f_m and gradually decreases with increasing f . The decrease begins at smaller f/f_m in the order of data No.3, No.1 and No.2, namely the order of increasing f_m , in accordance with the general features of coherence mentioned first in this section.

The theoretical values of coherence are also shown in the same figures (smooth curves). As regards the directional distribution, we assume $m=2, 4, 8$ to compute the cross spectrum and coherence. Figure 5 shows that the coherences predicted by the linear theory are fairly close to the measured ones for each pair of wave gauges if we select an adequate value of m .

It is difficult to determine the most suitable value of m for the measured ocean waves from Figure 5. Longuet-Higgins et al (1963) has proposed the following form of the angular distribution function;

$$G(\omega, \theta) = \frac{2^{2s-1}}{\pi} \frac{\Gamma^2(s+1)}{\Gamma(2s+1)} \left| \cos \frac{\theta}{2} \right|^{2s} \quad (7)$$

Recently, Mitsuyasu et al (1975) have determined an empirical formula for the parameter s in (7) as

$$s = 11.5 \left(\frac{2\pi f U}{g} \right)^{-2.5} \quad \text{for } f > f_m, \quad (8)$$

where U is wind velocity. By taking an approximate relation

$$m = 0.46s, \quad (9)$$

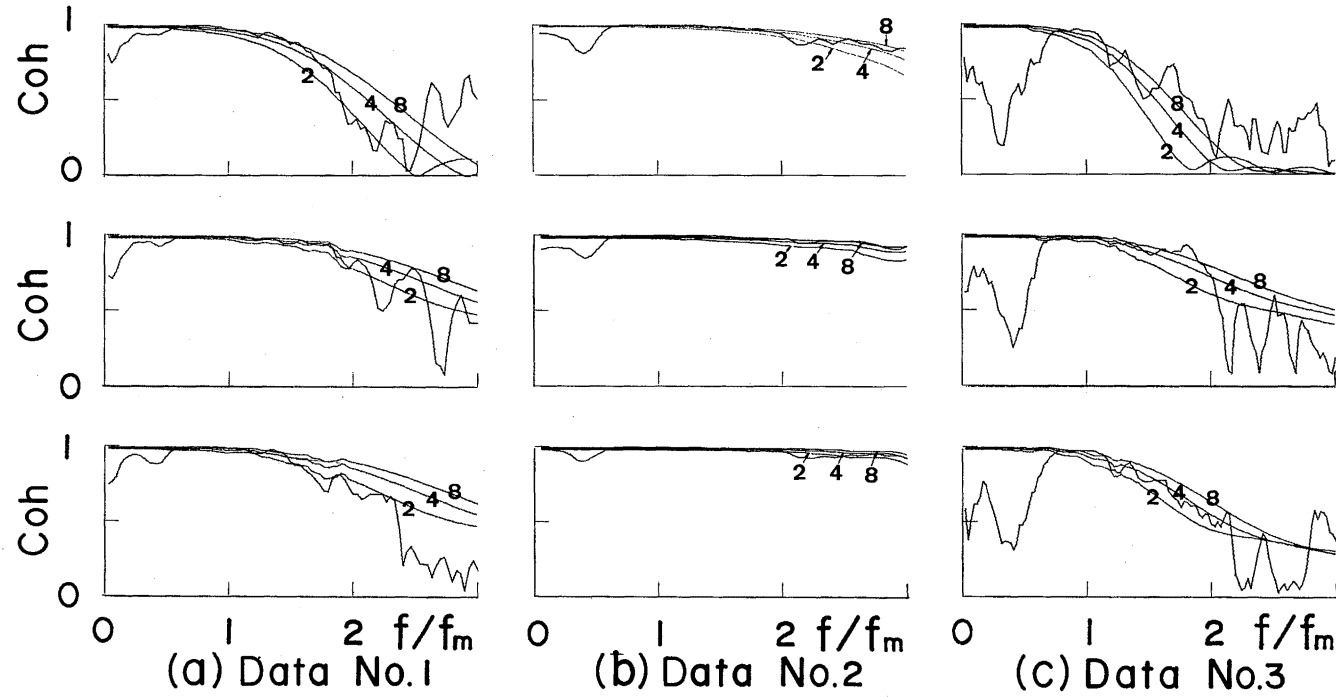


Figure 5, Comparison of the observed coherence (rugged line) with the prediction of the linear theory (smooth line), where the angular distribution function is assumed as $S(\theta) \sim \cos^m \theta$, $m=2, 4, 8$. The top, middle and bottom figures correspond respectively to the pairs of wave gauges 1-2, 2-3, and 3-1.

into account, we obtain

$$m = 5.29 \left(\frac{2\pi f U}{g} \right)^{-2.5}, \quad (10)$$

except for very small values of s ($s < 4$). The peak frequencies f_m of the present spectra give $m=8$ for data No.1 and $m=4$ for data No.3, which are consistent with observations. Since data No.2 corresponds to the swell, m can not be estimated from (10), which has been determined for ocean waves in generation area. According to Figure 5b, the measured coherence is very close to the theoretical one estimated by assuming $m=8$.

4.4 Phase velocity

The normalized (pseudo) phase velocity \tilde{C}/C_0 is shown at the bottom of Figures 3a, b and c as a function of the normalized frequency f/f_m . The phase velocity predicted by the linear theory is also shown in the same figures, where the angular distribution functions is the same to those used for the computation of the coherence. Figure 3 shows a fairly good agreement between the theory and observations. However, near the spectral peak frequency, observed (pseudo) phase speeds are a little smaller than theoretical values calculated under the assumption of moderate directional distributions $m=2\sim 8$.

Now, let us consider the reasons why the realistic model holds rather well, and why \tilde{C}/C_0 are slightly smaller than the theoretical values. For that purpose, we must discuss several factors which may invalidate the realistic model and consequently affect the phase velocity of wind waves.

Surface drift current induced by the wind

The phase velocity of laboratory wind waves is much affected by the drift current (Kato 1974, Kuo, et al. 1979). However, for ocean wind waves such as wave data No. 1 and No. 3, the surface velocity of the drift current of the order $U_0=0.03 U$ (U : wind velocity) is at most 3% of the phase velocity of linear waves. As for the swell, the drift current becomes less important partly due to low wind speed and partly due to large phase speed of the swell. Therefore, we conclude that the effect of the drift current on the phase velocity of ocean waves is negligibly small.

Nonlinear forced waves

In our previous papers (Masuda et al 1979, Mitsuyasu et al 1979), we have studied the nonlinear effect on the (pseudo) phase velocity for random

waves. According to those studies, nonlinear forced waves have a large effect on the (pseudo) phase velocity, if their spectral densities are comparable to or greater than those of free waves. However, as shown in Figure 4 the spectral densities of the nonlinear forced waves are much smaller than those of the free waves. Therefore, referring to our previous study (Mitsuyasu et al 1979 Appendix), we can say that the effect of nonlinear forced waves on the phase velocity is negligible in our present wave data.

The current

The current was not measured when the present data were obtained. According to a measurement made in other times at this platform, the current is mainly of tidal origin with maximum speed of the order of 0.20m/s. The speed is only about 3% of the phase velocity of linear waves with frequency 0.3Hz. Consequently, we can neglect the effect of ocean current on the phase velocities of ocean waves for the present data

Reflected wave

At a distance of approximately 2km from the tower, there are natural beach and fishing-port facilities. Some portion of the wave energy may be reflected from them. Therefore, the effect of the reflected waves need to be considered when we investigate the phase velocity of the ocean waves measured at the observation tower.

The method for determining the effects of reflected waves on the phase velocity is described in Appendix B^{*)}. As shown in Appendix B, the effect of reflected waves on the phase velocity depends not only on reflection coefficient but also on the phase lag between incident waves and reflected waves. Following the method described in Appendix B, we estimate the reflection coefficient and the phase lag from the wave data measured by two separate wave gauges. Then we estimate the phase velocity of wave system co-existing with the reflected waves. The reflection coefficients of the wave components near the spectral peak frequency are estimated approximately as 1.5% for wave data No.1 and No.3, and 5% for wave data No.2. If we consider these reflection coefficients, the apparent phase velocities of the spectral components near the spectral peak are approximately 92% of the phase velocity C_0 for wave data No.1, and approximately 83% of C_0 for wave data No.3. Here, C_0 is the true phase velocity of linear waves. For

^{*)} Since we have no informations on the directional properties of reflected waves, the formulation in Appendix B is made under the assumption of long-crested waves. Therefore, the results will be used only for the order estimation of the effect of reflected waves.

wave data No.2, effect of the reflected waves on the apparent phase velocity is found to be negligible, which is due to the values of the phase lag between the incident waves and the reflected waves.

If we consider these effects of the reflected waves on the measured phase velocity, the agreements between the theory and observations shown in Figure 3 are much improved.

Finally, some remarks are added on the measured (pseudo) phase velocity shown in Figure 3c. In a dimensionless form \tilde{C}/C_0 takes smaller values than 1.0 in the low frequency side ($0.8f_m-f_m$) of the wave spectrum. Since we have used the data window in the spectral analysis, this discrepancy can not be attributed to the leakage effects in the spectral computations. The similar behavior of \tilde{C}/C_0 is found in Lake & Yuen (1978). This problem is left for future study.

5. Conclusions

The main conclusion of this study is stated as follows: Observed (pseudo) phase velocity and coherence of the ocean waves presented here are well described by the realistic model of two-dimensional random linear waves. Slight disagreements between them seem attributable to the effects of opposing waves reflected from the shore.

There are two reasons why we can expect the validity of the linear model for ocean waves. First, the steepness of wind waves in the ocean is not so large as that of the laboratory wind waves, and their nonlinearities are weaker. Secondly, the wind-generated surface current can not have a large effect on the phase velocity of ocean waves, because the former is much smaller than the latter.

In one example of the data, a notable discrepancy is found between the linear theory and measurements in the low frequency side of the spectrum. Further studies are required to clarify this phenomenon.

Finally it should be noted that the present conclusions based on data of deep water waves must be reserved for ocean waves in shallow water such as shoaling water where the nonlinearity is not necessarily small.

Acknowledgements

The ocean wave data used in this study were obtained in an oceanographic project entitled "A study on a stable platform for oceanographic research" under a grant from the Ministry of Education. The analysis of the wave data was made on FACOM 230-48 computer system at Research Institute for Applied Mechanics.

The authors wish to express their gratitude to Mr. K. Eto and Mr. T. Honda for their assistance in the wave observation, to Mr. M. Tanaka for

computer analysis of the wave data, and to Miss M. Hojo for typing the manuscript.

References

- 1) Goda, Y., Kishira, Y. and Kamiyama, Y.: Laboratory investigation on the overtopping Rate of seawalls by irregular waves, Rep. Port & Harbour Res. Inst. 14 No.4 (1975) 3.
- 2) Kato, H.: Calculation of the wave speed for a logarithmic drift current, Rep. Port & Harbour Res. Inst. 13 No.4 (1974) 3.
- 3) Kuo, Y.Y., Mitsuyasu, H. and Masuda, A.: Experimental study on the phase velocity of wind waves, Part 1 Laboratory wind waves, Rep. Res. Inst. Appl. Mech. Kyushu Univ., 27 No.83 (1979) 1.
- 4) Lake, B.M. and Yuen, H.: A new model for non-linear wind waves, Part 1, Physical model and experimental evidence, J. Fluid Mech. 88 (1978) 33.
- 5) Longuet-Higgins, M.S., Cartwright, D.E. and Smith, N.D.: Observations of the directional spectrum of sea waves using the motions of a floating buoy, Proc. Conf. Ocean Wave Spectra, Prentice-Hall (1963) 111.
- 6) Masuda, A., Kuo, Y.Y. and Mitsuyasu, H.: On the dispersion relation of random gravity waves, Part 1, Theoretical framework, J. Fluid Mech. 92 (1979) 717.
- 7) Mitsuyasu, H., Kuo, Y.Y. and Masuda, A.: On the dispersion relation of random gravity waves, Part 2, An Experiment, J. Fluid Mech. 92 (1979) 731.
- 8) Mitsuyasu, H., Tasai, F., Suhara, T., Mizuno, S., Ohkusu, M., Honda, T. and Rikiishi, K.: Observations of the directional spectrum of ocean waves using a cloverleaf buoy, J. Phys. Oceanogr. 5 (1975) 750.
- 9) Tasai, F., Suhara, T., Mitsuyasu, H., Kawatate, K., Mizuno, S., Ohkusu, M., Koterayama, W., Tomioka, M., Hiyama, H., Nagahama, T., Arakawa, H., Honda, T., Takaki, M. and Masuda, A.: A study on a stable platform for oceanographic research (1), Bull. Res. Inst. Appl. Mech. No.46 (1977) 17 (in Japanese)
- 10) Yefimov, V.V., Solov'yev, Yu. P. and Khristoforov, G.N.: Observational determination of the phase velocities of spectral components of wind waves, IZV. Atmos. Oceanic Phys. 8 (1972) 435.

(Received July 5, 1979)

[**Appendix A**] Coherence and “pseudo” phase velocity predicted by the “realistic” model.

Consider a wave field described by the “realistic” model introduced in § 3.2. Then, the cross spectrum based on two wave gauges turns out to be

$$C_r(\omega) \equiv CO - iQU = \phi(\omega) \int_{-\pi}^{\pi} S(\omega, \theta) e^{-ik(\omega)l \cos(\theta - \beta)} d\theta, \quad (\text{A-1})$$

where $\phi(\omega)$ denotes the power spectrum and $k(\omega)$ the wavenumber defined by $k(\omega) \equiv \omega/C(\omega)$ with $C(\omega)$ the “true” phase speed. Here β is the direction of the two wave gauges and l the distance between them. The directional distribution $S(\omega, \theta)$ is of $\cos^m \theta$ -type with the main direction $\alpha(\omega)$. Rewriting (A-1) we have

$$\frac{C_r(\omega)}{\phi(\omega)} = \frac{1}{\sqrt{\pi}} \frac{\Gamma(1+m/2)}{\Gamma(1/2+m/2)} \int_{-\pi/2}^{\pi/2} \cos^m \theta e^{-ik(\omega)l \cos[\theta - (\beta - \alpha)]} d\theta. \quad (\text{A-2})$$

Next let us define the “pseudo” phase speed $\tilde{C}(\omega)$ by

$$\tilde{C}(\omega) = \omega l \cos(\beta - \alpha) / \tan^{-1} \left(\frac{QU}{CO} \right), \quad (\text{A-3})$$

which is not determined uniquely by the wave field but depends on the experimental conditions β and l . Normalization by the true phase speed $C(\omega)$ gives

$$\frac{\tilde{C}(\omega)}{C(\omega)} = k(\omega) l \cos(\beta - \alpha) / \tan^{-1} \left(\frac{QU}{CO} \right). \quad (\text{A-4})$$

Equations (A-2) and (A-4) indicate that the coherence $\text{Coh} \equiv |C_r(\omega)|/\phi(\omega)$ and normalized pseudo phase velocity $\tilde{C}(\omega)/C(\omega)$ are functions of $k(\omega)l$, the normalized distance of the wave gauges and $(\beta - \alpha)$, the direction of the wave gauges relative to the main wave direction.

Figures A-1 and A-2 respectively show Coh and \tilde{C}/C for $|\beta - \alpha| = 0^\circ, 20^\circ, 40^\circ, 60^\circ, 80^\circ$. The figures (a), (b), (c) and (d) correspond to $m = \infty, m = 8, m = 4$ and $m = 0$ (square distribution) respectively. Note that if $m = \infty$, the realistic model is reduced to the ideal one. Dimensional frequencies f are added to the figures for comparison with observations, where $k(\omega)l$ ($l = 7\text{m}$) is translated into f under the assumption of the linear dispersion relation $C(\omega) = C_0(\omega) = g/(2\pi f)$.

The contents of the “realistic” model are summarized in these figures. A glance tells us many features: (1) for $m = \infty$ (the ideal model), \tilde{C}/C and Coh are unity irrespective of $k(\omega)l$ or $|\beta - \alpha|$; (2) for finite m , \tilde{C}/C and Coh

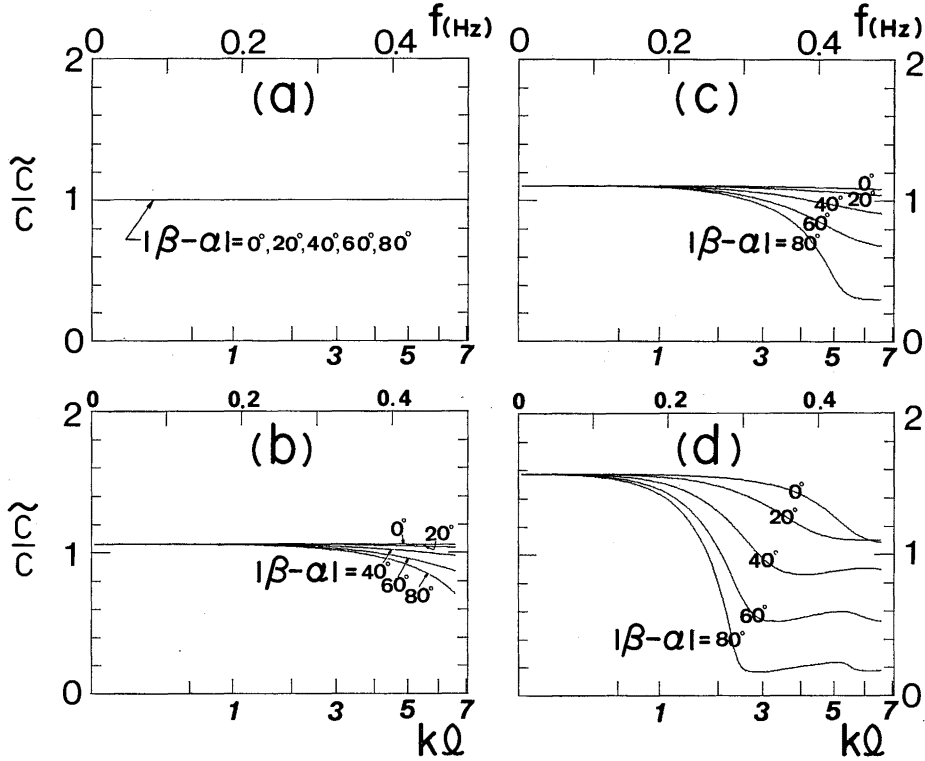


Figure A-1 The normalized "pseudo" phase velocity \tilde{C}/C predicted by (A-4) versus kl or f . $|\beta-\alpha|$ is taken as a parameter.
(a) $m=\infty$, (b) $m=8$, (c) $m=4$, (d) $m=0$

depend on both $k(\omega)l$ and $|\beta-\alpha|$; (3) departure from the ideal model becomes remarkable for smaller m , larger $k(\omega)l$ and larger $|\beta-\alpha|$; (4) As functions of $k(\omega)l$, \tilde{C}/C and Coh are almost constant ($\tilde{C}/C > 1$, $\text{Coh} \approx 1$) for small $k(\omega)l$ even in case of small m and large $|\beta-\alpha|$; (5) For any $|\beta-\alpha|$ the limit value of \tilde{C}/C as $k(\omega)l \rightarrow 0$ is equal to 1.0 when $m=\infty$, increases monotonically as m decreases and attains the maximum $\pi/2$ at $m=0$.

Finally a remark is stated about the error of the pseudo phase speed $\tilde{\delta C}$ produced when a slightly wrong value of the main direction $\alpha + \delta\alpha$ is used in the definition (A-3). We easily find, to the second order,

$$\frac{\tilde{\delta C}}{\tilde{C}} \sim (\delta\alpha) \tan(\beta-\alpha) - \frac{1}{2}(\delta\alpha)^2. \quad (\text{A-5})$$

It shows that the smaller the quantity $|\beta-\alpha|$, the smaller the error $\tilde{\delta C}$

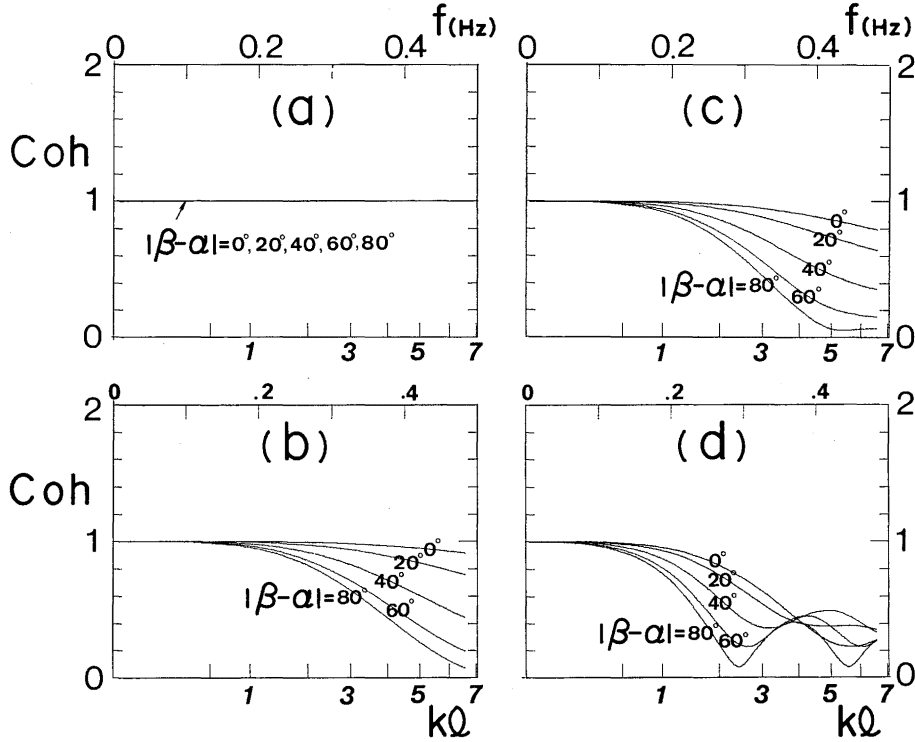


Figure A-2 Same as Figure A-1 except for coherence.

expected. Therefore experimentally the most reliable estimation of \tilde{C} is likely to be obtained with a pair of wave gauges parallel to the main direction.

[**Appendix B**] An effect of the reflected waves on the determination of wave velocity.

We consider a wave system which consists of two waves propagating to opposite directions, an incident wave and a reflected wave;

$$\eta(x, t) = a_i \cos(\omega t - kx + \varepsilon_i) + a_r \cos(\omega t + kx + \varepsilon_r), \quad (\text{B-1})$$

where a_i and ε_i are the amplitude and phase angle for the incident wave, and a_r and ε_r for the reflected wave. The cross-spectrum of waves $\eta(x_0, t)$ and $\eta(x_0 + l, t)$ measured at two stations separated by l in the x -direction can be determined by the Fourier analysis of the measured wave profile. From the cross spectrum the phase lag $\bar{\theta}$ is obtained as

$$\begin{aligned}\tan \bar{\theta} &= \frac{QU}{CO} = \frac{(a_i^2 - a_r^2) \sin kl}{(a_i^2 + a_r^2) \cos kl + 2a_i a_r \cos(2kx_0 - \varepsilon_i + \varepsilon_r + kl)} \\ &= R(a_r/a_i, 2kx_0 - \varepsilon_i + \varepsilon_r, kl),\end{aligned}\quad (\text{B-2})$$

where CO is the Co-spectrum and QU is the Quadrature spectrum.

It is easily seen that when the reflected wave is absent, the phase lag $\bar{\theta}$ becomes simply

$$\bar{\theta} = kl. \quad (\text{B-3})$$

We define an pseudo phase velocity \tilde{C} as

$$\tilde{C} = \omega l / \tan^{-1} R. \quad (\text{B-4})$$

Its normalized value is given by

$$\frac{\tilde{C}}{C_0} = \frac{kl}{\tan^{-1} R}, \quad (\text{B-5})$$

where $C_0 = \omega/k$.

The unknown quantities a_i , a_r and $(2kx_0 - \varepsilon_i + \varepsilon_r)$ in (B-2) can be determined through the Fourier analysis of the measured wave profiles after Goda (1975) as

$$a_i^2 = \frac{1}{4 \sin^2 kl} \left\{ \left(A_2 - A_1 \cos kl - B_1 \sin kl \right)^2 + \left(B_2 + A_1 \sin kl - B_1 \cos kl \right)^2 \right\}, \quad (\text{B-6})$$

$$a_r^2 = \frac{1}{4 \sin^2 kl} \left\{ \left(A_2 - A_1 \cos kl + B_1 \sin kl \right)^2 + \left(B_2 - A_1 \sin kl - B_1 \cos kl \right)^2 \right\}. \quad (\text{B-7})$$

and $\cos(2kx_0 - \varepsilon_i + \varepsilon_r)$

$$= \frac{1}{2a_i a_r} \left\{ a_i^2 + a_r^2 - \left(\frac{A_2 - A_1 \cos kl}{-\sin kl} \right)^2 + \left(\frac{B_2 - B_1 \cos kl}{\sin kl} \right)^2 \right\}. \quad (\text{B-8})$$

Here A_1 and B_1 are the Fourier coefficients of cosine component and sin component respectively for the waves measured at station x_0 , and so are A_2 and B_2 for the waves measured at station $x_0 + l$. Also for random waves, we can determine in the same way the reflection coefficient a_r^2/a_i^2 and the normalized apparent phase velocity \tilde{C}/C_0 as the functions of the frequency ω . Although equations (B-6), (B-7) and (B-8) have singular points at $\sin kl = 0$, we can eliminate the term $\sin kl$ and avoid the singular point as far as the reflection coefficient a_r^2/a_i^2 and the normalized phase velocity \tilde{C}/C_0 are concerned.